

# The piezoresistance coefficients of copper and copper-nickel alloys

CHANGYI HU, YIQUN GAO

*Institute of Precious Metals, Kunming 650221, People's Republic of China*  
*E-mail: ipm97cs@public.km.yn.cn*

ZHONGYI SHENG

*Institute of Physics, Chinese Academy of Sciences, Beijing 100080, People's Republic of China*

This paper attempts to further a better understanding of the piezoresistance coefficients by studying the piezoresistive effects in copper and copper-nickel alloys. The experimental evidence of isotropic piezoresistance coefficients ( $\pi_{11} = \pi_{12}$ ) has been obtained for the annealed copper and copper-nickel alloys. The piezoresistance coefficients of the cold-worked copper and Cu<sub>60</sub>Ni<sub>40</sub> alloy are of the tensor character ( $\pi_{11} \neq \pi_{12}$ ). A physical explanation has been given to the change of the ( $\pi_{ij}$ ) tensor. © 2000 Kluwer Academic Publishers

## 1. Introduction

Most of the studies of piezoresistive effects are focused on the usable stress-sensitive elements, e.g., ytterbium, manganin, constantan etc. In these papers, however, different authors reported different values of the piezoresistance coefficients ( $\pi_{11}$  and  $\pi_{12}$ ) and different relationships between  $\pi_{11}$  and  $\pi_{12}$  even for the same material. For instance, Chen [1] got the result of  $\pi_{11} \neq \pi_{12}$  for ytterbium, manganin and constantan. But Grady [2] and Neubert [3] obtained the relationship  $\pi_{11} = \pi_{12}$  for ytterbium and constantan respectively. Moreover, Neubert had ever mentioned that from experimental evidence there is no justification in assuming an isotropic piezoresistive coefficient in the elastic strain regime [3].

The present work had two main objectives (a) to investigate from the experimental evidence whether the isotropic piezoresistance coefficients ( $\pi_{11} = \pi_{12}$ ) exist by researching the piezoresistive effects in copper and copper-nickel alloys (b) to show the effects of the material states on the piezoresistance coefficients. Although the piezoresistance coefficients of copper and Cu<sub>60</sub>Ni<sub>40</sub> (constantan) can be found in literatures, yet some data needed to calculate the piezoresistance coefficients came from various sources. In this work, in order to obtain more reliable results, full sets of data are measured by ourselves under similar conditions and from the same material.

## 2. Theoretical aspects of the approach used

The general expression for the resistivity change induced by the stress for a material of cubic symmetry or higher takes the form [4]

$$\begin{bmatrix} \Delta\rho_1/\rho_0 \\ \Delta\rho_2/\rho_0 \\ \Delta\rho_3/\rho_0 \\ \Delta\rho_4/\rho_0 \\ \Delta\rho_5/\rho_0 \\ \Delta\rho_6/\rho_0 \end{bmatrix} = \begin{bmatrix} \pi_{11} & \pi_{12} & \pi_{12} & 0 & 0 & 0 \\ \pi_{12} & \pi_{11} & \pi_{12} & 0 & 0 & 0 \\ \pi_{12} & \pi_{12} & \pi_{11} & 0 & 0 & 0 \\ 0 & 0 & 0 & \pi_{44} & 0 & 0 \\ 0 & 0 & 0 & 0 & \pi_{44} & 0 \\ 0 & 0 & 0 & 0 & 0 & \pi_{44} \end{bmatrix} \begin{bmatrix} \sigma_1 \\ \sigma_2 \\ \sigma_3 \\ \sigma_4 \\ \sigma_5 \\ \sigma_6 \end{bmatrix} \quad (1)$$

where  $\rho_0$  is the strain-free resistivity,  $\Delta\rho_i/\rho_0$  ( $i = 1-6$ ) is the resistivity change,  $\sigma_i$  is the stress and  $\pi_{ij}$  is the piezoresistance coefficient. We choose the length of the wire along the  $x$  direction, then the first, second and third equations from the expansion of Equation 1 can be written

$$\frac{\Delta\rho_x}{\rho_0} = \pi_{11}\sigma_x + \pi_{12}\sigma_y + \pi_{12}\sigma_z \quad (2)$$

$$\frac{\Delta\rho_y}{\rho_0} = \pi_{12}\sigma_x + \pi_{11}\sigma_y + \pi_{12}\sigma_z \quad (3)$$

$$\frac{\Delta\rho_z}{\rho_0} = \pi_{12}\sigma_x + \pi_{12}\sigma_y + \pi_{11}\sigma_z \quad (4)$$

Thus, under the uniaxial tension stress conditions ( $\sigma_x \neq 0, \sigma_y = \sigma_z = 0$ ), we obtain

$$\frac{\rho_x}{\rho_0} = \pi_{11}\sigma_x = \pi_{11}E\varepsilon_L \quad (5)$$

where  $\varepsilon_L$  is the longitudinal strain in the wire and  $E$  is the Young's modulus.

Under the hydrostatic stress conditions ( $\sigma_x = \sigma_y = \sigma_z = -p$ ), we get the expression for the resistivity change

$$\left(\frac{\Delta\rho}{\rho_0}\right)_{\text{HS}} = (\pi_{11} + 2\pi_{12})(-P) \quad (6)$$

where  $P$  is the pressure.

Combining the definitions of the elastic strain sensitivity of resistance  $\eta$  ( $\eta = (\Delta R/R_0)/\varepsilon_L$ ) and the pressure coefficient of resistance  $K_{\text{HS}}$  ( $K_{\text{HS}} = (\Delta R/R_0)/P$ ), we can finally obtain the following two expressions for  $\eta$  from Equations 5 and 6, as in ref. [5]

$$\eta = 1 + 2\mu + \pi_{11}E \quad (7)$$

$$\eta = 2 - E(K_{\text{HS}} + 2\pi_{12}) \quad (8)$$

where  $\Delta R/R_0$  is the relative resistance change and  $\mu$  is the Poisson's ratio. In order to obtain the data of  $\pi_{11}$  and  $\pi_{12}$  from Equations 7 and 8, the data of  $\eta$ ,  $K_{\text{HS}}$ ,  $\mu$  and  $E$  should be measured experimentally.

### 3. Experimental details and results

#### 3.1. Preparation of samples

Copper and nickel metals, with a purity greater than 99.95%, were melted in an alumina crucible and poured into a graphite mould. The ingots were drawn into 10.2 and 0.102 mm in diameters for determining  $E$ ,  $\mu$  and  $\eta$ ,  $K_{\text{HS}}$  respectively. The heat treatment conditions and cold-worked reductions of the samples are summarized in Table I. The compositions of the samples were identified by chemical analysis.

#### 3.2. Hydrostatic tests for the pressure coefficients of resistance

The definition of pressure coefficient of resistance is  $K_{\text{HS}} = [\Delta R/R_0]_{\text{HS}}/P$ , where  $[\Delta R/R_0]_{\text{HS}}$  is the relative change of resistance under the hydrostatic pressure  $P$ . Fig. 1 is the schematic diagram of an apparatus for the measurements of the relative resistance change with pressure. The medium for pressure transmission is a kind of mixed oil being of good electric insulation prop-

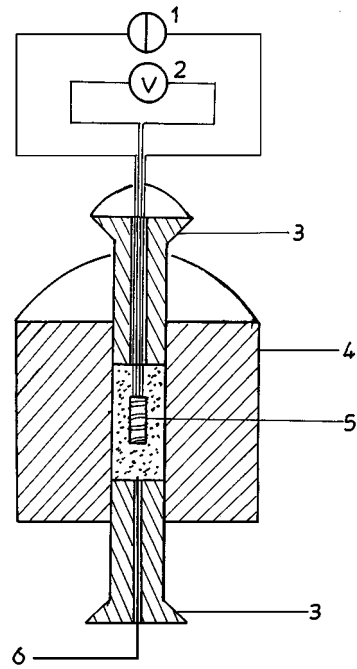


Figure 1 Schematic diagram of an apparatus for measuring relative resistance changes of metals and alloys under hydrostatic pressure. (1) Constant current source, (2) volt-ohm-milliammeter, (3) pistons, (4) cylinder, (5) sample, (6) thermocouple.

erty. The sample wire were wound non-inductively on a pyrophyllite cylinder. The lengths of the wires were from 300 to 1000 mm which were determined in terms of the resistivity of the wires. The data of resistance were obtained by measuring the voltage and the current which was kept constant. A thermocouple was used to inspect the temperature in the pressure chamber.

The relationships between the resistance ratio  $R_p/R_0$  ( $R_p$  and  $R_0$  are the resistance under pressure  $P$  and atmosphere respectively) and the pressure  $P$  are shown in Figs 2 and 3. The pressure coefficients of resistance  $K_{\text{HS}}$  are determined from these figures. The data of  $K_{\text{HS}}$  and the errors are summarized in Table II.

#### 3.3. Uniaxial loading tests for the elastic strain sensitivity of resistance

The definition of  $\eta$  is  $\eta = (\Delta R/R_0)/(\Delta L/L_0)$ , where  $\Delta R/R_0$  is the relative resistance change of a sample wire under the uniaxial strain ( $\Delta L/L_0$ ). The schematic

TABLE I States of samples

| Sample number | Samples                           | Annealed conditions |            |                      |            | Cold-worked reductions of area (%) |
|---------------|-----------------------------------|---------------------|------------|----------------------|------------|------------------------------------|
|               |                                   | 10.2 mm in diameter |            | 0.102 mm in diameter |            |                                    |
|               |                                   | Temp (°C)           | Time (min) | Temp (°C)            | Time (min) |                                    |
| 1             | Cu                                | 550                 | 25         | 540                  | 15         |                                    |
| 2             | Cu <sub>98</sub> Ni <sub>2</sub>  | 650                 | 30         | 630                  | 15         |                                    |
| 3             | Cu <sub>94</sub> Ni <sub>6</sub>  | 650                 | 40         | 630                  | 15         |                                    |
| 4             | Cu <sub>92</sub> Ni <sub>8</sub>  | 700                 | 30         | 680                  | 15         |                                    |
| 5             | Cu <sub>80</sub> Ni <sub>20</sub> | 750                 | 30         | 730                  | 15         |                                    |
| 6             | Cu <sub>60</sub> Ni <sub>40</sub> | 800                 | 30         | 760                  | 15         |                                    |
| 7             | Cu <sub>50</sub> Ni <sub>50</sub> | 800                 | 35         | 760                  | 15         |                                    |
| 8             | Cu                                |                     |            |                      |            | 83                                 |
| 9             | Cu <sub>60</sub> Ni <sub>40</sub> |                     |            |                      |            | 57                                 |

TABLE II The values and the correspondent errors of  $E$ ,  $\mu$ ,  $\eta$ ,  $K_{HS}$ ,  $\pi_{11}$  and  $\pi_{12}$  for copper and copper-nickel alloys

| Sample number | Material state | $E$ (GPa) | $\mu$ | $\eta$          | $K_{HS} \times 10^3$ (GPa) $^{-1}$ | $\pi_{11} \times 10^3$ (GPa) $^{-1}$ | $\pi_{12} \times 10^3$ (GPa) $^{-1}$ |
|---------------|----------------|-----------|-------|-----------------|------------------------------------|--------------------------------------|--------------------------------------|
| 1             | Annealed       | 121       | 0.353 | $2.39 \pm 0.05$ | $-15.9 \pm 0.2$                    | $5.7 \pm 0.5$                        | $6.3 \pm 0.6$                        |
| 2             | Annealed       | 127       | 0.348 | $2.25 \pm 0.05$ | $-11.0 \pm 0.1$                    | $4.4 \pm 0.5$                        | $4.5 \pm 0.6$                        |
| 3             | Annealed       | 130       | 0.348 | $2.14 \pm 0.06$ | $-7.32 \pm 0.06$                   | $3.4 \pm 0.5$                        | $3.1 \pm 0.6$                        |
| 4             | Annealed       | 131       | 0.346 | $2.00 \pm 0.04$ | $-4.3 \pm 0.1$                     | $2.4 \pm 0.4$                        | $2.2 \pm 0.5$                        |
| 5             | Annealed       | 144       | 0.334 | $2.05 \pm 0.04$ | $-5.96 \pm 0.05$                   | $2.7 \pm 0.3$                        | $2.8 \pm 0.4$                        |
| 6             | Annealed       | 160       | 0.329 | $2.02 \pm 0.03$ | $-4.72 \pm 0.04$                   | $2.3 \pm 0.3$                        | $2.3 \pm 0.4$                        |
| 7             | Annealed       | 168       | 0.325 | $2.02 \pm 0.03$ | $-4.3 \pm 0.1$                     | $2.2 \pm 0.2$                        | $2.1 \pm 0.3$                        |
| 8             | Cold-worked    | 119       | 0.339 | $2.85 \pm 0.09$ | $-8.5 \pm 0.3$                     | $10 \pm 1$                           | $1 \pm 2$                            |
| 9             | Cold-worked    | 160       | 0.322 | $2.3 \pm 0.1$   | $-5.9 \pm 0.4$                     | $4.1 \pm 0.7$                        | $2.0 \pm 0.9$                        |

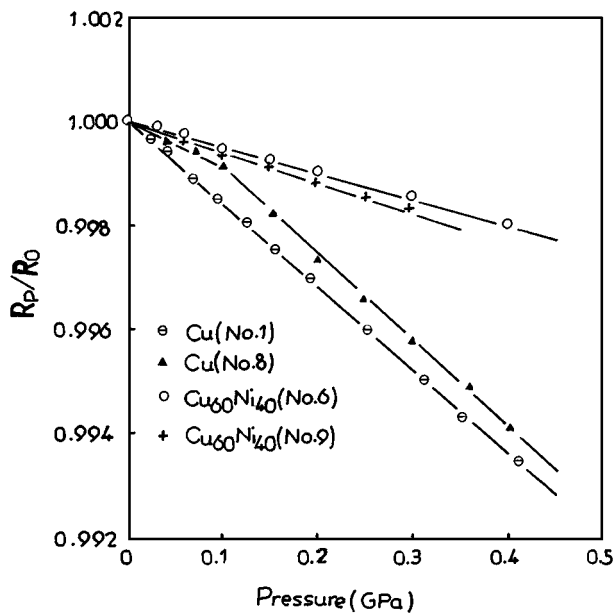


Figure 2 The changes in resistance ratio  $R_p/R_0$  with hydrostatic pressure of annealed and cold-worked Cu and  $Cu_{60}Ni_{40}$  wires.

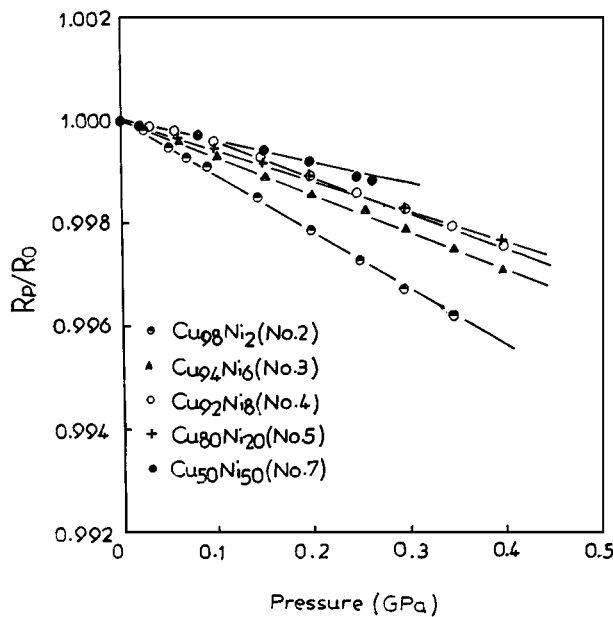


Figure 3 The changes in resistance ratio  $R_p/R_0$  with hydrostatic pressure of annealed  $Cu_{98}Ni_2$ ,  $Cu_{94}Ni_6$ ,  $Cu_{92}Ni_8$ ,  $Cu_{80}Ni_{20}$  and  $Cu_{50}Ni_{50}$  wires.

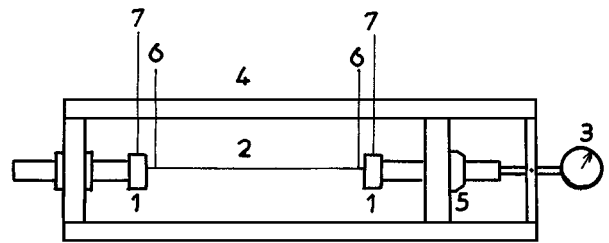


Figure 4 Schematic diagram of an apparatus for measuring relative resistance changes of sample wires under uniaxial elongation condition. (1) Clamps, (2) sample wire, (3) micrometer, (4) frame, (5) nuts, (6) voltage leads, (7) current leads.

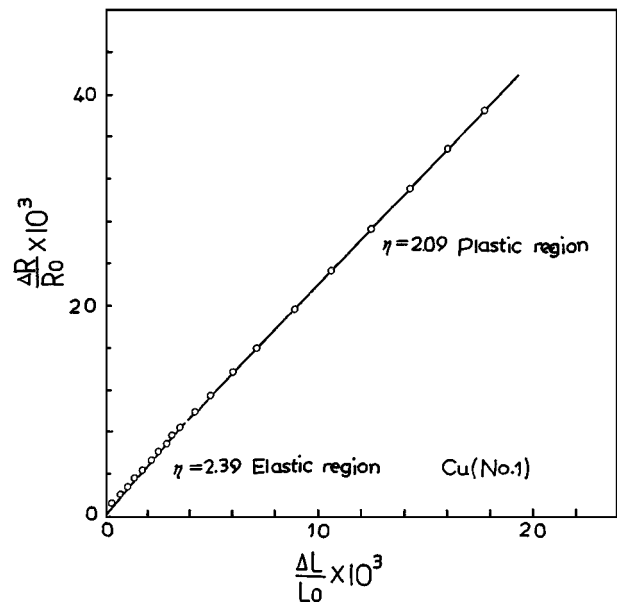


Figure 5 The changes in resistance ratio  $\Delta R/R_0$  with longitudinal strain  $\Delta L/L_0$  of annealed Cu wire.

view of the setup for measuring  $\eta$  is shown in Fig. 4. The original length of the sample wires were about 280 mm. The electrical resistance was measured by a kelvin-type double bridge and the strain of the wires was determined by a micrometer with an accuracy of 0.001 mm.

The typical changes in electrical resistance ratio with longitudinal extension are shown in Figs 5–8. The broken points in the curves are the yield points. The elastic strain sensitivity of resistance and the errors are listed in Table II.

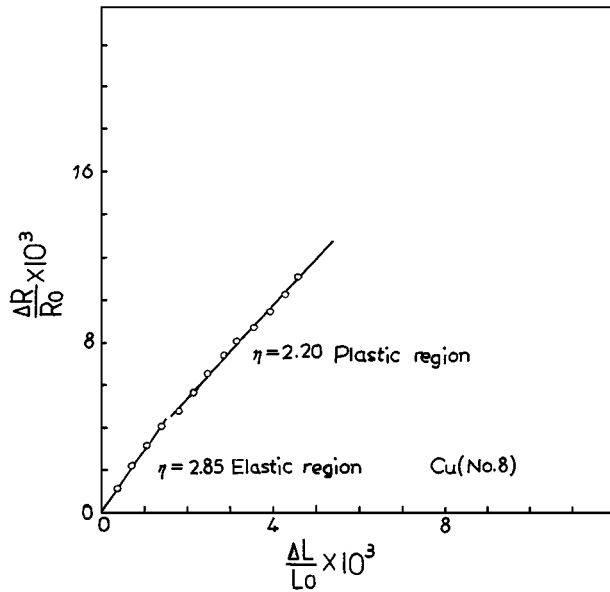


Figure 6 The changes in resistance ratio  $\Delta R/R_0$  with longitudinal strain  $\Delta L/L_0$  of cold-worked Cu wire.

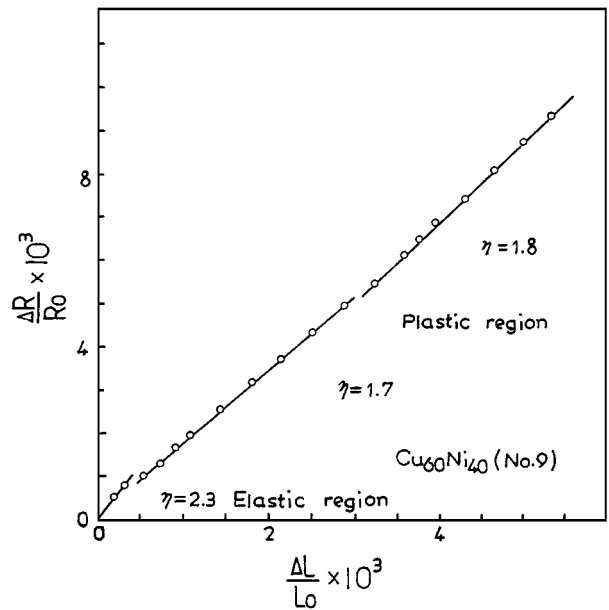


Figure 8 The changes in resistance ratio  $\Delta R/R_0$  with longitudinal strain  $\Delta L/L_0$  of cold-worked  $\text{Cu}_{60}\text{Ni}_{40}$  wire.

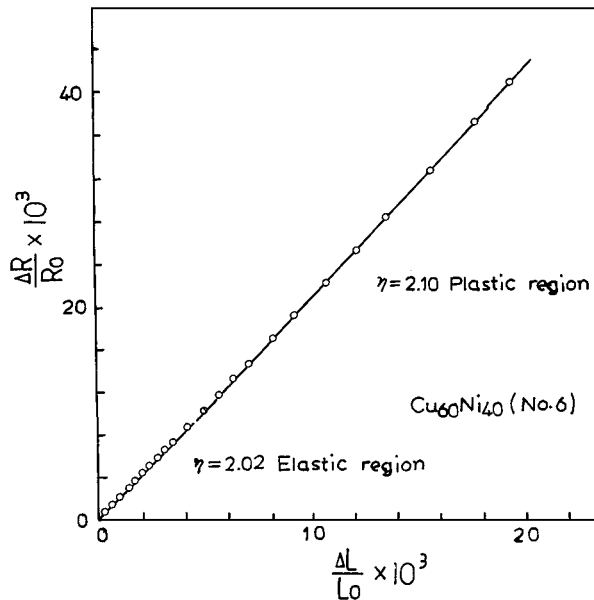


Figure 7 The changes in resistance ratio  $\Delta R/R_0$  with longitudinal strain  $\Delta L/L_0$  of annealed  $\text{Cu}_{60}\text{Ni}_{40}$  wire.

### 3.4. The measurements of Young's modulus and Poisson's ratio

The Young's modulus and Poisson's ratio were determined by ultrasonic method. The transmission velocity of ultrasonic waves in a metal is closely related to its elastic modulus  $E$ , Poisson's ratio  $\mu$  and density  $d$ . For isotropic metals, the relationships are expressed by the following equations [6].

$$E = \frac{d(3V_1^2V_s^2 - 4V_s^4)}{(V_1^2 - V_s^2)} \quad (9)$$

$$\mu = \frac{(V_1^2 - 2V_s^2)}{(2V_1^2 - V_s^2)} \quad (10)$$

where  $V_1$  and  $V_s$  are the longitudinal and transverse wave velocity respectively. In this work,  $V_1$  and  $V_s$  were measured by ultrasonic method which was described in detail in reference [6]. The determination of  $E$  and  $\mu$  are more complicated for anisotropic metals. For simplification, we assume that the cold-worked Cu and  $\text{Cu}_{60}\text{Ni}_{40}$  are of cubic symmetry and the longitudinal direction of the wire is [100]. Then the elastic stiffness  $C_{11}$  can be expressed as follows [7]:

$$C_{11} = dV_1^2 \quad (11)$$

$C_{11}$  is related to  $E$  and  $\mu$  by Equation (12) [8]

$$C_{11} = \frac{E(1 - \mu)}{[(1 + \mu)(1 - 2\mu)]} \quad (12)$$

The values of  $E$  and  $d$  were determined by dynamic resonance method [9] and Archimedes principle respectively. Then the values of  $\mu$  were obtained from Equations 11 and 12. The data of Young's modulus and Poisson's ratio are listed in Table II.

### 4. Piezoresistance coefficients

Substituting the experimental data of  $K_{HS}$ ,  $\eta$ ,  $E$  and  $\mu$  into Equations 7 and 8, we obtained the two independent piezoresistance coefficients  $\pi_{11}$  and  $\pi_{12}$  which are presented in Table II. The evaluation of the errors of  $\pi_{11}$  and  $\pi_{12}$  is of great importance for the present paper to come into reliable conclusions. The experimental errors of the data have been taken into account carefully and then the absolute errors of  $\pi_{11}$  and  $\pi_{12}$  are obtained in terms of the error theory.

The errors in  $E$  and  $\mu$  of all the samples are  $\pm 1$  and  $\pm 0.001$  respectively.

We can see from Table II that the two independent coefficients of each annealed metal or alloy are equal in the range of the experimental error. Thus, the present work

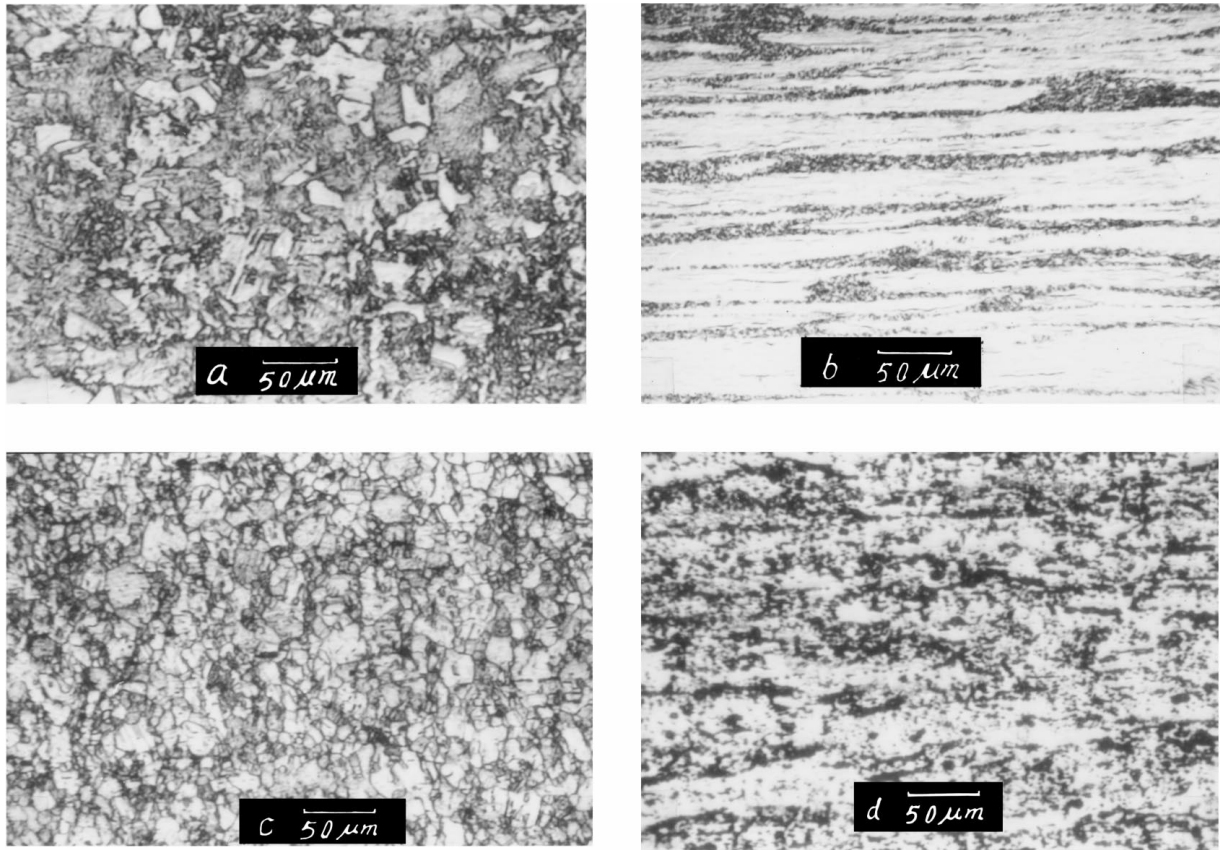


Figure 9 The metallographs of annealed Cu (No. 1) (a), cold-worked Cu (No. 8) (b), annealed Cu<sub>60</sub>Ni<sub>40</sub> (No. 6) (c) and cold-worked Cu<sub>60</sub>Ni<sub>40</sub> (No. 9) (d).

has furthered an experimental evidence of isotropic piezoresistance coefficients. While for cold-worked Cu and Cu<sub>60</sub>Ni<sub>40</sub> alloy,  $\pi_{11}$  is not equal to  $\pi_{12}$ .

The microstructure observations have been had for the annealed and cold-worked materials. The typical metallographs of Cu and Cu<sub>60</sub>Ni<sub>40</sub> alloy are shown in Fig. 9. The annealed materials can be treated as the isotropic media because their crystals are random orientations. Thus, the three independent piezoresistance coefficients satisfy the isotropic condition [2]

$$\pi_{44} = \pi_{11} - \pi_{12}$$

According to this condition, we can obtain  $\pi_{44} = 0$  for the annealed materials examined in the present work. Therefore, the tensor of the piezoresistance coefficients can be reduced to a scalar. In contrast, the cold-worked Cu and Cu<sub>60</sub>Ni<sub>40</sub> alloy are anisotropic materials because of the textured structure induced by the cold processing. Thus, the resistivity of them is related to the direction of the crystals. As a result, the piezoresistance coefficient of the cold-worked Cu and Cu<sub>60</sub>Ni<sub>40</sub> must be a tensor according to Equation 1.

We have ever mentioned that different researchers obtained different results about the piezoresistance coefficients even for the same material. The cause of the phenomenon may be that the data needed to calculate the piezoresistance coefficients come from various sources or the material state is different because the processing of the material results in the change in the form of the  $(\pi_{ij})$  tensor in terms of the present work.

## 5. Concluding remarks

In the present paper, the two independent piezoresistance coefficients  $\pi_{11}$  and  $\pi_{12}$  of copper and copper-nickel alloys have been determined by measuring the full set of the experimental data needed to calculate them. We arrive at the following conclusions:

1. We obtained  $\pi_{11} = \pi_{12}$  in the range of the experimental errors for annealed copper and copper-nickel alloys. This result has furthered an experimental evidence of isotropic piezoresistance coefficients.
2. The two independent piezoresistance coefficients are not equal each other for the cold-worked Cu or Cu<sub>60</sub>Ni<sub>40</sub> alloy. The tensor properties of the piezoresistance effects in these cold-worked materials cannot be ignored. The textured structure of the cold-worked materials results in the change in the form of the  $(\pi_{ij})$  tensor.

## Acknowledgements

Senior engineers F. Y. Li, T. Z. Deng and Z. T. Zhang of Institute of Physics of Chinese Academy of Sciences are sincerely thanked for their great help to our experiments. Mr. Du of Institute of Precious Metals is also thanked for his help in the preparation of the samples.

## References

1. D. Y. CHEN, Y. M. GUPTA and M. H. MILES, *J. Appl. Phys.* **55** (1984) 3984.
2. D. E. GRADY and M. J. GINSBERG, *ibid.* **48** (1977) 2179.

3. H. K. P. NEUBERT, The Elasto-Resistive Effect in Metal Wires and Films, AD703304 (1969).
4. C. S. SMITH, *Solid State Phys.* **6** (1962) 197.
5. Z. ROSENBERG, *Mater. Sci. Eng.* **100** (1988) L9.
6. F. BIRCH, *J. Geophys. Research* **66** (1961) 2199.
7. H. M. LEDBETTER and D. T. READ, *J. Appl. Phys.* **48** (1977) 1874.
8. G. JOOS, "Theoretical Physics," (London, 1958) p. 181.
9. E. SCHREIBER, O. L. ANDERSON and N. SOGA, "Elastic Constants and Their Measurement," (1973) p. 100.

*Received 27 July 1998  
and accepted 14 June 1999*